

## Fluid Dynamics Simulation of a Pilot-Scale Solid-State Fermentation Bioreactor

Diego R. Pessoa<sup>a</sup>, Anelize T. J. Finkler<sup>a</sup>, Alex V. L. Machado<sup>a</sup>, Luiz Fernando L. Luz Jr.<sup>a</sup>, David A. Mitchell<sup>b</sup>

<sup>a</sup>Universidade Federal do Paraná, Departamento de Engenharia Química, Caixa Postal 19011 – Centro Politécnico – CEP 81531-980 – Curitiba – Paraná – Brasil

<sup>b</sup>Universidade Federal do Paraná, Departamento de Bioquímica e Biologia Celular, Caixa Postal 19046 – Centro Politécnico – CEP 81531-980 – Curitiba – Paraná – Brasil  
[diego.pes@hotmail.com](mailto:diego.pes@hotmail.com)

Solid-state fermentation (SSF) has potential advantages for the production of certain biotechnological products, due to its large volumetric productivity and low operating costs. However, there are major challenges in obtaining adequate heat and mass transfer when this fermentation method is used at large scales. Mathematical models and computer simulations are useful tools for designing strategies to overcome these challenges, given the cost of large-scale fermentation experiments. In the current work, we used the commercial CFD software ANSYS FLUENT® 16.0 to develop a mathematical model for heat and mass transfer in a pilot-scale packed-bed bioreactor. The model takes into account the dynamics of airflow in the porous substrate bed and the lack of thermal and moisture equilibrium between the solid and gas phases. The permeability parameters were obtained from pressure drop measurements made in the pilot-scale bioreactor during a fermentation in which *Aspergillus niger* was grown on a mixture of wheat bran and sugar cane bagasse. The CFD simulations were able to represent the temperature and moisture profiles observed experimentally during the initial heating of the substrate bed by the process air. A parametric analysis was also performed, in order to understand better the physical dynamics of the system. Our work provides the basis for the development of a robust and reliable model for testing operating conditions and control strategies for large-scale cultivation in SSF bioreactors.

### 1. Introduction

Despite the growing interest in producing microbial products by solid-state fermentation (SSF), there are major challenges to face when using this cultivation method at large-scale, due to the relatively poor heat and mass transfer within the bed of solid particles. Mathematical models and computational simulations are useful tools for developing operating and control strategies to overcome these challenges. It is therefore surprising that, to date, there are few examples of the application of computational fluid dynamics (CFD) to SSF bioreactors. CFD models can predict radial temperature and mass transfer gradients in complex geometries of flow. Additionally, current commercial CFD packages allow easy visualization and analysis of the results in 3D.

Recently, we studied the production of pectinases by *Aspergillus niger* in a pilot-scale packed-bed bioreactor, using a porous substrate bed consisting of wheat bran (WB) and sugarcane bagasse (SCB), in a 90:10 mass ratio (Pitol *et al.*, 2016). The aim of the current work was to develop a CFD simulation of heat and mass transfer in this bed, thereby providing the basis for the development of a model that can, in the future, be used as a tool for identifying appropriate operating strategies for optimizing the performance of cultivations undertaken in this bioreactor. Experimental pressure drop data were collected in the pilot-scale bioreactor, in order to obtain the permeability coefficients characterizing the resistance of the porous substrate bed. The simulations were validated with experimental data for bed temperature and moisture content obtained during the initial heating of the bed by the process air.

### 2. Model development and materials and methods

#### 2.1 Model of heat and mass transfer in the bed of solid particles

We used the model for heat and water transfer in porous SSF beds proposed by von Meien and Mitchell (2002). This model considers the solid and gas phases separately, with differential equations being used to

describe the balances on water and energy in these phases. This model has provided good descriptions for heat and water transfer in the pilot-scale bioreactor used by Pitol *et al.* (2016), as shown by experiments undertaken in the absence of microbial growth by Marques *et al.* (2006), although this investigation did not recognize the heterogeneity of the porous medium, nor the presence of radial profiles. The equations were inserted into the commercial CFD software ANSYS Fluent® 16.0 through UDF's (user defined functions).

The model of von Meien and Mitchell (2002) was developed for the growth of *A. niger* on corn. We replaced the equation for the isotherm of corn used by von Meien and Mitchell (2002) with the equation of Peleg (1993), proposed by Casciatori *et al.* (2015) to fit to the isotherm of wheat bran and sugar cane bagasse:

$$\varphi_s^* = P_1 a_{wg}^{P_2} + P_3 a_{wg}^{P_4} \quad (1)$$

In this equation, the fitting constants  $P_1$ ,  $P_2$ ,  $P_3$  and  $P_4$  were 0.117, 0.364, 0.522 and 8.342, respectively, for wheat bran and 0.145, 10.98, 0.107 and 1.058, respectively, for sugarcane bagasse (Casciatori *et al.*, 2015).

## 2.2 Solid-state fermentation experiments

The bed of solids was 0.4 m high and had a porosity of 0.564 (calculated using Eq(7) and Eq(8) in Table 1). It had an initial temperature of 25.6°C and an initial moisture content of 1.50 kg/kg (dry basis). The inlet air had a temperature of 32.0°C and a water activity of 0.99 and was supplied at a flow rate of 0.077 kg/s.

## 2.3 Calculation of parameters

Through the pressure drop correlation from ANSYS, it is possible to fit experimental data in order to obtain the viscous (1/K) and inertial resistance ( $C_2$ ) coefficients for a porous medium or a membrane (porous-jump):

$$\left(\frac{\Delta P}{L}\right) = \frac{\mu}{K} v + \frac{\rho C_2}{2} v^2 \quad (2)$$

The remaining properties of the substrate solids as functions of moisture content (MC) are estimated as shown in Table 1. Note that MC refers to the moisture content on a wet basis and the specific heat capacity of the 9:1 mixture of wheat bran and sugarcane bagasse was taken as that of 100 % wheat bran.

Table 1: WB and SCB moist particle and porous bed parameters as a function of moisture content (MC).

Parameter	Material	Equation/Value		Source
Solid particle density (kg/m <sup>3</sup> )	WB	0.974 + 0.226MC	Eq(3)	Casciatori <i>et al.</i> (2014)
	SCB	0.578 + 0.00365exp $\left(\frac{MC}{0.149}\right)$	Eq(4)	Casciatori <i>et al.</i> (2014)
Solid specific heat capacity (J/(kg. °C))*	WB	1590.0		Sweat (1986)
Solid thermal conductivity (W/(m. °C))	WB	0.213 + 0.264MC	Eq(5)	Casciatori <i>et al.</i> (2013)
	SCB	16.8 – 35.7 · 0.51 $\frac{1}{MC}$	Eq(6)	Casciatori <i>et al.</i> (2013)
Solid bulk porosity on Loose Packing	WB	0.91 – 0.016exp $\left(\frac{MC}{0.30}\right)$	Eq(7)	Casciatori <i>et al.</i> (2014)
	SCB	0.62 – 0.136MC	Eq(8)	Casciatori <i>et al.</i> (2014)

Note: \*estimated by weighted average with the actual moisture content.

## 2.4 Pressure drop data

The pressure drop data used for calculation of the permeability coefficients were obtained from experiments in the pilot-scale packed bed-bioreactor, undertaken as described by Pitol *et al.* (2016). Wheat bran and sugarcane bagasse were used (on a dry mass basis, 27 kg and 3 kg, respectively). The pressure drop was measured with a mercury manometer connected to the bioreactor air inlet and outlet. Pressure drop data was obtained for five different airflow rates between 170.7 and 252.5 m<sup>3</sup>/h.

## 2.5 Bioreactor geometry

The bioreactor, located at the Federal University of Paraná, is as described by Pitol *et al.* (2016). The dimensions were measured and the 3D geometry was drawn using ANSYS ICEM CFD® 16.0 and exported to

ANSYS Fluent® 16.0. A hexahedral mesh with minimum determinant 2x2x2 quality of 0.325 and 66,495 nodes was generated (Figure 1a). The experimental temperature measurements were provided by thermocouples installed inside the substrate chamber at three different heights ( $z$ ) (Table 2). The thermocouple locations are related to the origin point at the inferior corner of the empty substrate chamber (indicated by “0” in Figure 1a) and the bioreactor air inlet and outlet are also indicated in Figure 1a.

A highly refined, inflated tetrahedral mesh was developed for the perforated plate in order to estimate its flow resistance coefficients. The flow of air at different superficial velocities was simulated, providing estimates of pressure drop across the plate. A curve was fitted to this data, enabling estimation of the inertial and viscous coefficients of Eq(2). These coefficients were used in the porous-jump (Table 3).

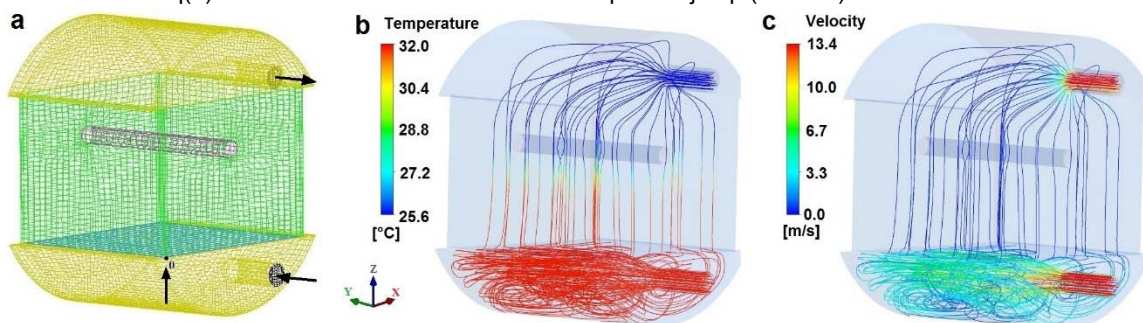


Figure 1: Bioreactor geometry: a – Mesh; b – Temperature streamlines; c – Velocity streamlines.

Table 2: Thermocouple positions: the  $y$  positions are given in the same order as the thermocouple labels in the column headings.

	T1; T2; T0; T3	T4; T7; T5; T6	T11; T10; T9; T8
x (cm)	65	14	27
y (cm)	9.0; 29.5; 42.5; 55.0	6.0; 16.0; 30.5; 47.5	10.0; 22.0; 27.5; 44.5
z (cm)	5	18	33

## 2.6 Mesh analysis

In the first mesh analysis, we isolated the porous bed geometry to see the effect of three different mesh refinements and time step values on the quality of the results of the model simulation. The porous bed volume was about 0.177 m<sup>3</sup> and the low, medium and high refinements resulted in average element volumes of 7.29, 3.40 and 1.27 cm<sup>3</sup>, respectively. The time steps tested were 0.1, 0.01 and 0.001 s. In the second analysis, we tested the influence of the three refinements and four different turbulence models (laminar, k-epsilon, k-omega and transition k-kl-omega) on the airflow distribution through the porous-jump. The bioreactor volume was about 0.395 m<sup>3</sup> and the low, medium and high refinements resulted in average element volumes of 6.46, 2.58 and 1.15 cm<sup>3</sup>, respectively. The turbulence models were tested at steady state and simulations stopped at default convergence criteria or when they reached 1,200 iterations. Meshes with even lower refinements were not an option because they led to non-realistic bioreactor geometry with poor quality elements.

## 2.7 Parametric analysis

The parameters presented in Sections 2.1 and 2.2 and Table 3 represent the central case simulation. Parameters were varied relative to this central case: airflow 20 % higher, solid specific heat 20% lower, particle density 20 % lower, porous medium heat transfer coefficient 20 % lower and bed porosity 20 % higher.

## 3. Results

### 3.1 Pressure drop and permeability

For five different airflow rates, the pressure drop varied between 1,831.6 and 2,830.7 Pa/m. Curve fitting gave a viscous coefficient ( $1/K$ ) of  $5.12 \times 10^8 \text{ m}^{-2}$  and an inertial resistance coefficient ( $C_2$ ) of  $19,340 \text{ m}^{-1}$ . Pressure drop data (8 points) were also collected during the first 10 h of the fermentation at a constant air flow rate of 240 m<sup>3</sup>/h (0.077 kg/s). The pressure drop oscillated between 761.2 and 1712.7 Pa/m, with an average value of 1,308.3 Pa/m. The values of air density (1.16 kg/m<sup>3</sup>) and viscosity ( $2.81 \times 10^{-5} \text{ Pa}\cdot\text{s}$ ) used to calculate the resistance coefficients were for the average operating temperature of 29.3 °C (Perry and Green, 1999).

### 3.2 Mesh Analysis

The refinement of the substrate mesh had little influence on the quality of the simulation results. The minimum refinement quality set was based on the 2x2x2 determinant quality criterion equal to 0.3, the minimum value required by the Fluent® simulator. However, the size of the time step affected the results. Time steps of 0.01 and 0.001 s gave quite similar temperatures and air and substrate moisture profiles, with poor quality results being obtained with a time step size of 0.1 s. Therefore a 0.01 s time step was chosen for the simulations.

With respect to turbulence model, both 2-equation models (k-epsilon and k-omega) had low computational cost requirements and gave airflow distribution results similar to those obtained with the transition 3-equation model. The k-epsilon model was chosen because it gave a smooth behavior for the evaporation rate profile whereas both the k-omega model and the transition model gave oscillatory behavior.

The effect of the chamber mesh refinement on the symmetry of the flow distribution pattern through the porous-jump was investigated. The gas enters below the porous-jump in the Y direction. The flow hits the opposite wall and the turbulence generated helps to distribute the flow throughout the inferior chamber. Figure 2 shows the resulting z velocity flow through the porous-jump surface. The low and medium refinements produced similarly asymmetric patterns; only the most refined mesh produced a symmetric flow pattern (Figure 2). However, the highly refined mesh is overly time consuming. Since the mesh refinement had relatively little influence on the simulation results, the low refinement was chosen for the simulations, as it allowed for faster simulations. Figure 1c shows the resulting simulated air flow through the bioreactor.

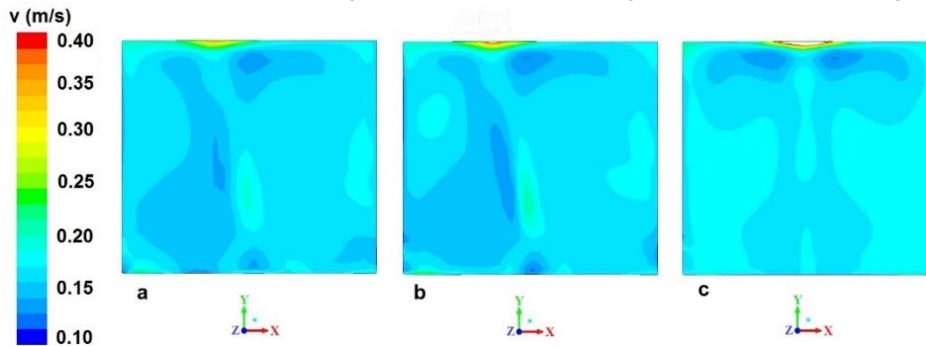


Figure 2: Flow distribution pattern through porous-jump obtained with different refinements: a – low; b – medium; c – high.

### 3.3 Simulation settings, simulations and parametric analysis

The substrate bed was represented as a homogenous porous medium and the perforated base plate was treated as a porous wall (porous-jump) in order to reduce the computational cost, while maintaining the quality of the results (Prukwarun *et al.*, 2013). A pressure drop across the porous bed of 1,175.5 Pa/m was estimated through the simulation, which is close to the average value obtained experimentally in the first 10 h (i.e. before growth of the fungal mycelium into the inter-particle spaces). Table 3 gives the main parameters and simulation settings.

Table 3: Description of simulation settings.

Description	Method/Value
Moist solids particle density (kg/m <sup>3</sup> )	1,077
Moist solids specific heat capacity (J/(kg.°C))	3,146.4
Moist solids thermal conductivity (W/(m.°C))	0.3536
Porous medium thermal mode	Non-equilibrium
Heat transfer coefficient (W/(m <sup>2</sup> .°C))	58,376.7*
Operating pressure (Pa)	101,325
Porous jump parameters	1/K= 2.88 x 10 <sup>6</sup> m <sup>2</sup> ; L = 0.002 m; C <sub>2</sub> = 15,578.7 1/m
Time step (s)	0.01

\*Interpolated values from Lima (2009) for gas temperature of 305 K.

Temperature profiles during bed heating were measured for three bed heights (z values) (symbols in Figure 3). Each curve represents the average of the values recorded by the thermocouples at that height.

Lower heights are heated first, such that the curves begin to rise in the order  $z=5$  cm, then  $z=18$  cm and, finally,  $z=33$  cm. Figure 1b shows the temperature streamlines of the air for the flowtime of 600 s: there is a short region of temperature transition (where the streamline changes from red to blue) inside the substrate bed. The height within the bed at which this transition occurs gradually increases over time. The simulated temperature profiles do not agree perfectly with the experimental ones (Figure 3a), with the greatest difference being that, experimentally, the profile for  $z=18$  cm begins to rise much earlier than predicted.

The parametric analysis shows that, with exception of the heat transfer coefficient, all of the parameters affected the predicted heating curves noticeably. The reduction of the bed specific heat allowed the curves to rise earlier, as the reduction in particle density made it easier to heat the system (Figure 3b). With increased bed porosity, the heating curves were dislocated to the left (Figure 3c); this is expected, since higher void fractions should imply reduced bulk density and thus reduced thermal inertia. A higher air flow rate dislocated the curves significantly to the left, while a reduced heat transfer coefficient had little effect (Figure 3d).

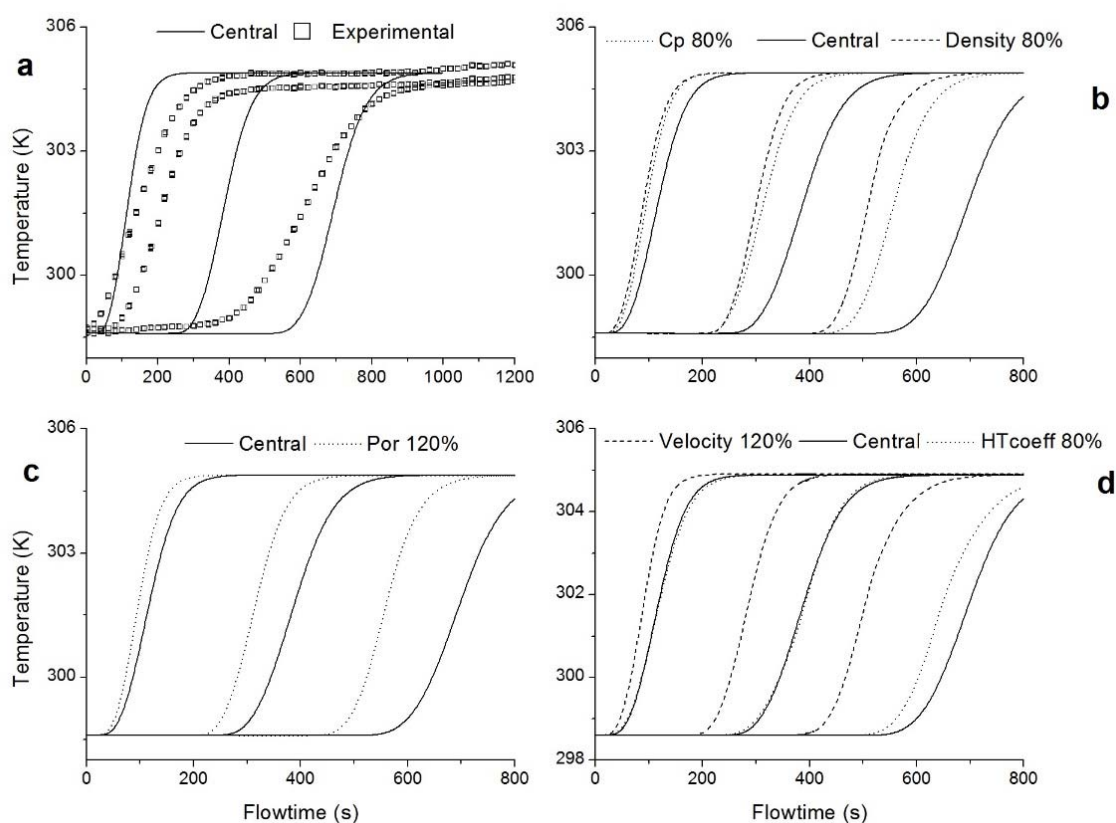


**Figure 3: Simulated temperature profiles and parametric analysis. Comparison: a - experimental data and central simulation; b - central, substrate specific heat ( $C_p$ ) 20 % lower and particle density 20 % lower; c - central and substrate porosity ( $Por$ ) 20 % higher; d - central, airflow 20 % higher and substrate heat transfer coefficient ( $HT_{coeff}$ ) 20 % lower.**

The predicted moisture contents of the air and substrate are average values for XY planes perpendicular to the air flow direction. Figure 4 shows predictions for five different bed heights, including at the substrate surface ( $z=40$  cm). The moisture content of the air increases from 0.0205 kg/kg, corresponding to the initial condition of moisture equilibrium at 25.6 °C, to 0.0300 kg/kg, corresponding to a water activity of 0.99 at 32 °C. The substrate moisture content shows a similar behavior, but varies over a very narrow range (Figure 4). As the substrate is colder than the air and the gas phase is almost saturated, condensation of water occurs, increasing the moisture content of the substrate slightly (Figure 4). This condensation accelerates the substrate heating process since it is an exothermal phenomenon. As expected, in both profiles the lower heights suffer the variation earlier.

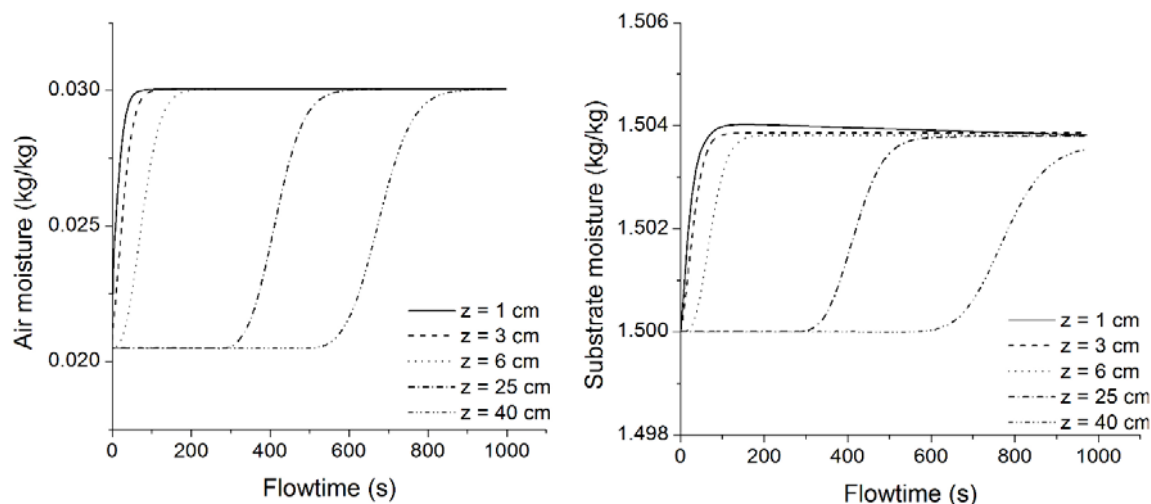


Figure 4: Predicted air and substrate moisture profiles.

#### 4. Conclusion

Despite some discrepancies, the CFD simulations gave reasonable descriptions of the dynamics of heat and water transfer within the porous bed composed of wheat bran and sugarcane bagasse. With the incorporation of a model for microbial growth, this CFD model could be extended to provide a robust and reliable tool for testing operating conditions and control strategies for large-scale cultivations in SSF bioreactors.

#### Nomenclature

$\varphi_s^*$	Solid moisture at equilibrium (kg/kg)	$\Delta P$	Pressure drop (Pa)
$a_{wg}$	Water activity of the gas phase	$L$	Porous medium thickness (m)
$\mu$	Fluid viscosity (Pa.s)	$K$	Permeability (m <sup>2</sup> )
$\rho$	Fluid density (kg/m <sup>3</sup> )	$C_2$	Inertial resistance coefficient (1/m)
$v$	Fluid superficial velocity (m/s)		

#### 5. References

- Casciadori F.P., Laurentino C.L., Lopes K.C.M., de Souza A.G., Thoméo J.C., 2013, Stagnant effective thermal conductivity of agro-industrial for solid-state fermentation. *Int. J. of Food Prop.* 16, 1578-1593.
- Casciadori F.P., Laurentino C.M., Taboga S.R., Casciadori P.A., Thoméo, J.C., 2014, Structural properties of beds packed with agro-industrial solid by-products applicable for solid-state fermentation: Experimental data and effects on process performance. *Chem. Eng. J.* 255, 214-224.
- Casciadori F.P., Laurentino C.L., Zanelato A.I., Thoméo J.C., 2015, Hygroscopic properties of solid agro-industrial by-products used in solid-state fermentation. *Ind. Crop. Prod.* 64, 114-123
- Lima T., 2009, Modelo de inferência para a estimação da umidade do leito de um biorreator de fermentação no estado sólido. Master's Thesis – UFPR, Curitiba-PR, Brazil.
- Marques B.C., Barga M.C., Balmant W., Luz Jr L.F.L., Krieger N., Mitchell D.A., 2006, A model of the effect of the microbial biomass on the isotherm of the fermenting solids in solid-state fermentation. *Food Technol. Biotechnol.* 44, 457-463.
- Peleg M., 1993. Assessment of a semi-empirical four parameter general model for sigmoid moisture sorption isotherms. *J. Food Process Eng.* 16, 21-37.
- Perry R.H. and Green D.W., 1999, Perry's chemical engineering handbook, USA, McGraw-Hill, p.2-208.
- Pitol L.O., Biz A., Mallmann E., Krieger N., Mitchell D.A., 2016, Production of pectinases by solid-state fermentation in a pilot-scale packed-bed bioreactor. *Chem. Eng. J.* 283, 1009-1018.
- Prukwarun W., Khumchoo W., Seancoth W., 2013, CFD simulation of fixed bed dryer by using porous media concepts: Unpeeled longan case. *Int. J. Agric. & Biol. Eng.* 6, 100-110.
- Sweat V.E. Thermal properties of foods. *Engineering properties of foods*. New York: Marcel Dekker, 1986.
- von Meien O.F. and Mitchell D.A., 2002, A two-phase model for water and heat transfer within an intermittently-mixed solid-state fermentation bioreactor with forced aeration. *Biotechnol. Bioeng.* 79, 416-28.